

Dynamic Phase-Shifting Electronic Speckle Pattern Interferometer

Michael North Morris, James Millerd, Neal Brock, John Hayes and *Babak Saif

4D Technology Corporation, 3280 E. Hemisphere Loop Suite 146, Tucson, AZ 85706
(520) 294-5600, (520) 294-5601 fax, michael.north-morris@4dtechnology.com

*Space Telescope Science Institute, Baltimore, MD

ABSTRACT

The technique for measuring changes in diffuse surfaces using Electronic Speckle Pattern Interferometry (ESPI) is well known. We present a new electronic speckle pattern interferometer that takes advantage of a single-frame spatial phase-shifting technique to significantly reduce sensitivity to vibration and enable complete data acquisition in a single laser pulse. The interferometer was specifically designed to measure the stability of the James Webb Space Telescope (JWST) backplane. During each measurement the laser is pulsed once and four phase-shifted interferograms are captured in a single image. The signal is integrated over the 9ns pulse which is over six orders of magnitude shorter than the acquisition time for conventional interferometers. Consequently, the measurements do not suffer from the fringe contrast reduction and measurement errors that plague temporal phase-shifting interferometers in the presence of vibration. This paper will discuss the basic operating principle of the interferometer, analyze its performance and show some interesting measurements.

Keywords: ESPI, Interferometer, Spatial Phase-Shifting, Dynamic, Speckle, JWST, Vibration Insensitivity

1. INTRODUCTION

The testing of the back-plane stability for primary telescope mirrors requires the measurement of large diffuse meter-class structures from a significant standoff location in the presence of vibration. Distance measuring interferometers are capable of measuring the surface deformation in one direction at discrete locations. However, the data is sparse and the technique requires attaching retro-reflectors to the structure under test which may distort the results. A better approach is to use Electronic Speckle Pattern Interferometry (ESPI). ESPI can measure the deformations of the entire surface simultaneously without attaching auxiliary optics to the test article^{1,2}. Although, combined with traditional phase-shifting techniques a speckle interferometer can make high resolution measurements³, the acquisition time is too slow to provide vibration immunity. The speckle interferometer presented here combines the ability to measure large diffuse structures with spatial phase shifting to overcome the speed limitations of traditional phase-shifting interferometry. The system is capable of measuring meter-class structures with an acquisition time of 9ns which is six orders of magnitude shorter than the acquisition time for conventional interferometers.

A variety of methods for spatial phase shifting have been developed over the years. The most common are the use of multiple cameras^{4,5}, the use of diffractive elements to simultaneously image three or more images onto a single CCD^{6,7} and the use of tilt to introduce a spatial carrier frequency to the pattern⁸. The multiple camera approach tends to be expensive and difficult to implement, it can be difficult to design fast imaging for the diffraction approach due to the off-axis beams produced by the diffractive element and the spatial carrier approach can be difficult to use in the presence of the speckle pattern.

The spatial phase shifting used here does not fall directly into any of the above categories. The four phase-shifted frames are simultaneously captured by placing a pixelated phase mask directly in front of the CCD that introduces a unique phase shift at each pixel. Pixelated phase shifting has the following advantages:

- 1) A true common path arrangement permits the use of broadband or white light
- 2) Extremely compact design
- 3) Achromatic over a wide range
- 4) Fixed spatial interference pattern results in fast processing

5) Single-frame data acquisition

2. MEASUREMENT TECHNIQUE

2.1 Simultaneous phase-shift measurement

At the heart of the speckle interferometer is a new spatial phase-shifting method in which four phase-shifted interferograms are simultaneously generated on a single CCD array. The optical layout of the interferometer is shown in figure 1. The test article is illuminated slightly off-axis with a high power pulsed Nd:YAG laser operating at the second harmonic (532nm). The pulse width of the laser is 9ns producing a coherence length of 2.7m. A small portion of the output beam is coupled into a polarization maintaining fiber which serves two purposes. First the fiber provides flexibility for directing the reference into the receiver unit and secondly the fiber provides a simple method for path matching the test and reference signals. By placing different lengths of fiber between the illumination head and the receiver unit it is possible to introduce the required time delay into the reference beam. A half-wave plate is placed in front of the fiber coupling to assist in the alignment of the incident polarization with the fast or slow axis of the fiber. The field of illumination for the test beam is controlled changing the separation between the illumination lenses. The test article is imaged onto the CCD via an imaging lens relay combination. The relay is added to provide space for the reference beam to be folded into the path and to control the speckle size on the CCD. The relay has an adjustable field stop that effectively changes the F/# of the imaging train. The reference beam is launched from the end of the fiber and collimated. After collimation it passes through a polarizer to clean up the polarization, a half-wave plate and a polarizing beam splitter into the path compensation adjustment arm of the receiver. The combination of the half-wave plate and the polarizing beam splitter provide a means for controlling the reference irradiance on the camera. The compensation arm is used to make fine adjustments on the path matching. The reference beam reflects off a flat mirror on a translation stage by way of a quarter-wave plate that is used to rotate the polarization of the reference beam 90 degrees. On the second pass through the beam splitter the reference beam is reflected into the optical path of the test beam and is focused through the adjustable stop in the relay and collimated before arriving at the CCD. The pixelated mask mounted directly in front of the CCD encodes a high spatial frequency interference pattern on the two orthogonally polarized test and reference beams as shown in figure 2. The phase mask is designed to have a one-to-one correspondence with the CCD that is to say that each pixel on the CCD receives an individually phase-shifted signal. The phase mask has four unique phase-shifts (ABCD) and is patterned so that every pixel is in quadrature with its neighbors. The phase difference between the test and reference arms is obtained using an N-bucket algorithm or spatial convolution.

Some of the advantages for ESPI applications of the pixelated approach to phase shifting are that the spatial interference pattern is fixed and that there is no varying spatial distortion between the four phase-shifted images.

2.2 Data Processing

Phase-shifted ESPI measurements are made by capturing two measurements one before and one after the surface is perturbed and subtracting the phase. The phase subtraction can be done directly in the phase domain; however, performing the subtraction in the interferogram domain before the arctangent is applied has the distinct advantage of facilitating the application of smoothing routines to reduce the sensitivity to random irradiance fluctuations. Although, the subtracting of two measurements significantly reduces the random irradiance pattern and enables the detection of correlation fringes, there is some speckle decorrelation between the frames resulting in fringes that are low contrast and noisy. Applying a smoothing function to the subtraction reduces the noise in the measurement and improves the contrast of the correlation fringes. The algorithm for performing the subtraction in the interferogram can be derived by applying the following trigonometric identity to the phase subtraction.

$$\tan(a - b) = \frac{\tan(a) - \tan(b)}{1 + \tan(a) \cdot \tan(b)} \quad (2.1)$$

The resulting Algorithm is

$$\Delta f_c = \text{ArcTan} \left(\frac{X(x, y)}{Y(x, y)} \right) \quad (2.2)$$

where

$$X(x, y) = [D_1(x, y) - B_1(x, y)] \cdot [A_2(x, y) - C_2(x, y)] - [A_1(x, y) - C_1(x, y)] \cdot [D_2(x, y) - B_2(x, y)]$$

$$Y(x, y) = [A_2(x, y) - C_2(x, y)] \cdot [A_1(x, y) - C_1(x, y)] + [D_1(x, y) - B_1(x, y)] \cdot [D_2(x, y) - B_2(x, y)]$$

A_1, B_1, C_1, D_1 are the phase-shifted interferograms for the baseline measurement and A_2, B_2, C_2, D_2 are the phase-shifted interferograms for the second measurement.

Noise in the measurement can be significantly reduced using a weighted spatial average over neighboring pixels. This can be accomplished by:

$$\Delta f_c(x, y) = \text{ArcTan} \left(\frac{\sum_{x, y \in d} X(x, y)}{\sum_{x, y \in d} Y(x, y)} \right), \quad (2.3)$$

where the sums are performed over a range of d nearest neighbors. Because of the modulo $2p$ behavior of the arctangent function, the range is wrapped (ambiguous) beyond the wavelength of the source. Any number of well known processes of spatial unwrapping can be used to remove the discontinuous steps and perform quantitative analysis of the interferograms.

2.2 Speckle Size Requirements

When considering the desired speckle size at the camera there are two competing factors that govern the selection; 1) throughput and 2) speckle decorrelation between the spatially offset pixels. The small spatial offset between the pixels used to calculate the phase leads to a difference in irradiance and phase between neighboring pixels. The larger the average speckle size relative the offset in the pixels the smaller the differences. The obvious solution is to stop down the imaging aperture to enlarge the speckle size; however, doing so has the adverse consequence of reducing the throughput of the imaging train. When measuring large structures light is at a premium and needs to be conserved whenever possible. A good compromise between these two competing factors is to match the mean speckle size to the "unit cell" (The extent of the

repeating pattern in the mask.) At this condition there is only a slight increase in the noise in the measurement for low fringe densities when compared to an extremely stable temporal phase-shifting measurement and there is practically no difference for higher fringe densities (0.2 fringes per pixel or greater.)⁹ It should be noted that in the presence of vibration the noise in the temporally phase-shifted measurement would far exceed the spatial phase-shifted measurement.

3. FREQUENCY RESPONSE

Dynamic interferometry implies the ability to make measurements in the presence of vibrations. The combination of spatial phase shifting and an extremely short integration time qualifies this interferometer as dynamic. The total integration time required to obtain all four phase-shifted frames is 9ns, over six orders of magnitude shorter than conventional interferometers.

The figure of merit for the dynamic performance of the speckle interferometer is the fringe contrast reduction. The fringe contrast limited frequency response can be estimated by examining the fringe contrast reduction of a specular measurement in the presence of a single vibrational frequency, f . The expression for good fringe contrast is expressed mathematically as follows;

$$\frac{8 \cdot p}{l} \cdot A \cdot \sin(p \cdot t \cdot f) \leq 2 \cdot p \tag{3.1}$$

and

$$t \ll \frac{1}{f}$$

where A is the radial amplitude of the vibration, t is the integration time for a single frame and l is the wavelength of light. Integrating the fringe pattern over the integration time using the maximum velocity of the vibration and calculating the fringe contrast leads to the following expression for the fringe contrast.

$$V = \text{Sinc} \left(\frac{4 \cdot A \cdot p^2 \cdot t \cdot f}{l} \right) \tag{3.2}$$

Figure 3 shows the frequency response when the contrast reduction is limited to 50%. The sloping segment of the line is the region where the fringe contrast is reduced due to phase changes during the integration time as described by equation (3.2), the plateau below 10KHz, represents the fringe contrast reduction due to the high fringe density on the CCD and the cutoff at 50MHz represents a reduction in fringe contrast resulting from the integration time approaching the period of the vibration.

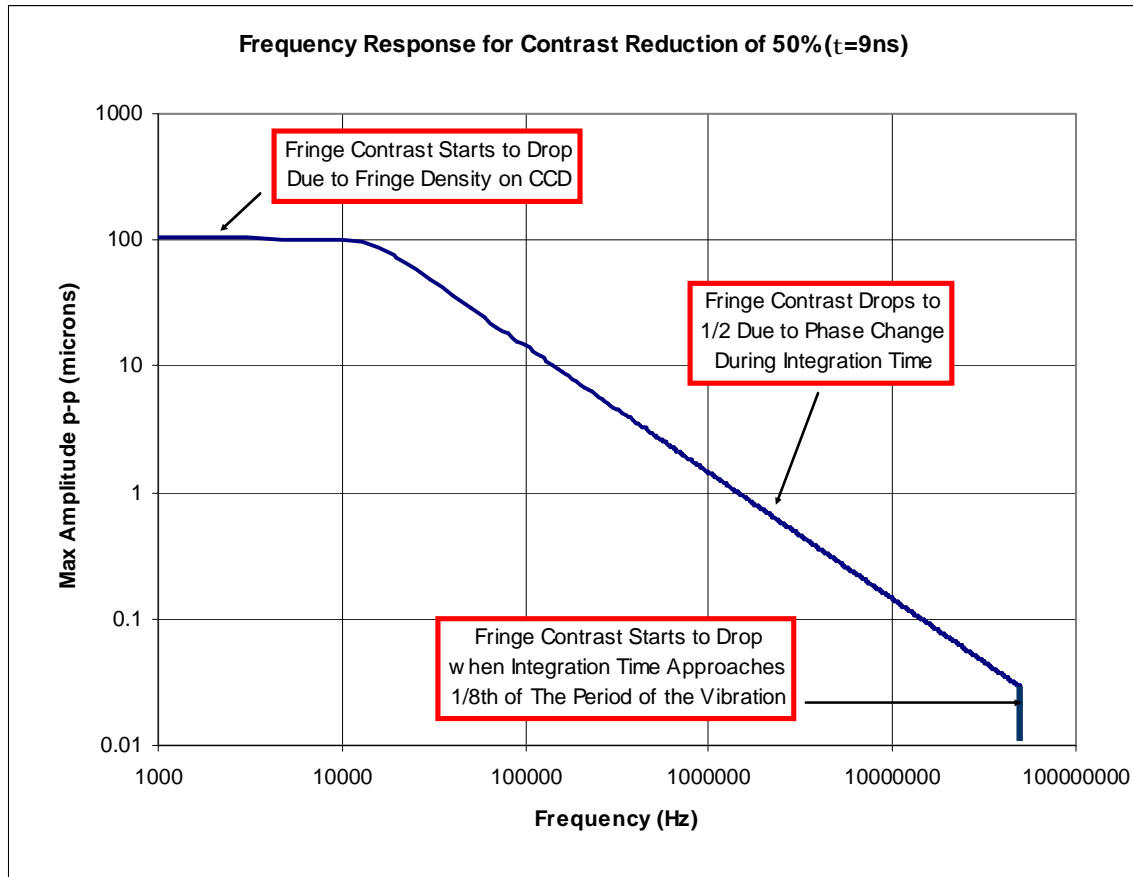


Figure 3: Fringe contrast limited frequency response

4. RESULTS

The operation of the interferometer was tested by measuring a 1 meter diameter target made of carbon fiber. The sample was illuminated and imaged off-axis with angle of 5 degrees between the laser and the receiver. The interferometer and the test article were placed on separate unisolated tables with a 4m standoff between the interferometer and the target. The test article was perturbed between measurements by pushing the center of the carbon fiber target toward the interferometer with a micrometer. The resulting wrapped phase is shown in figure 4 (the wrapped phase is typical of ESPI measurements made using the carrier fringe technique¹⁰) and the unwrapped phase for an average of 15 measurements is shown in figure 5.



Figure 4: Wrapped phase from measurement of a 1m carbon fiber target

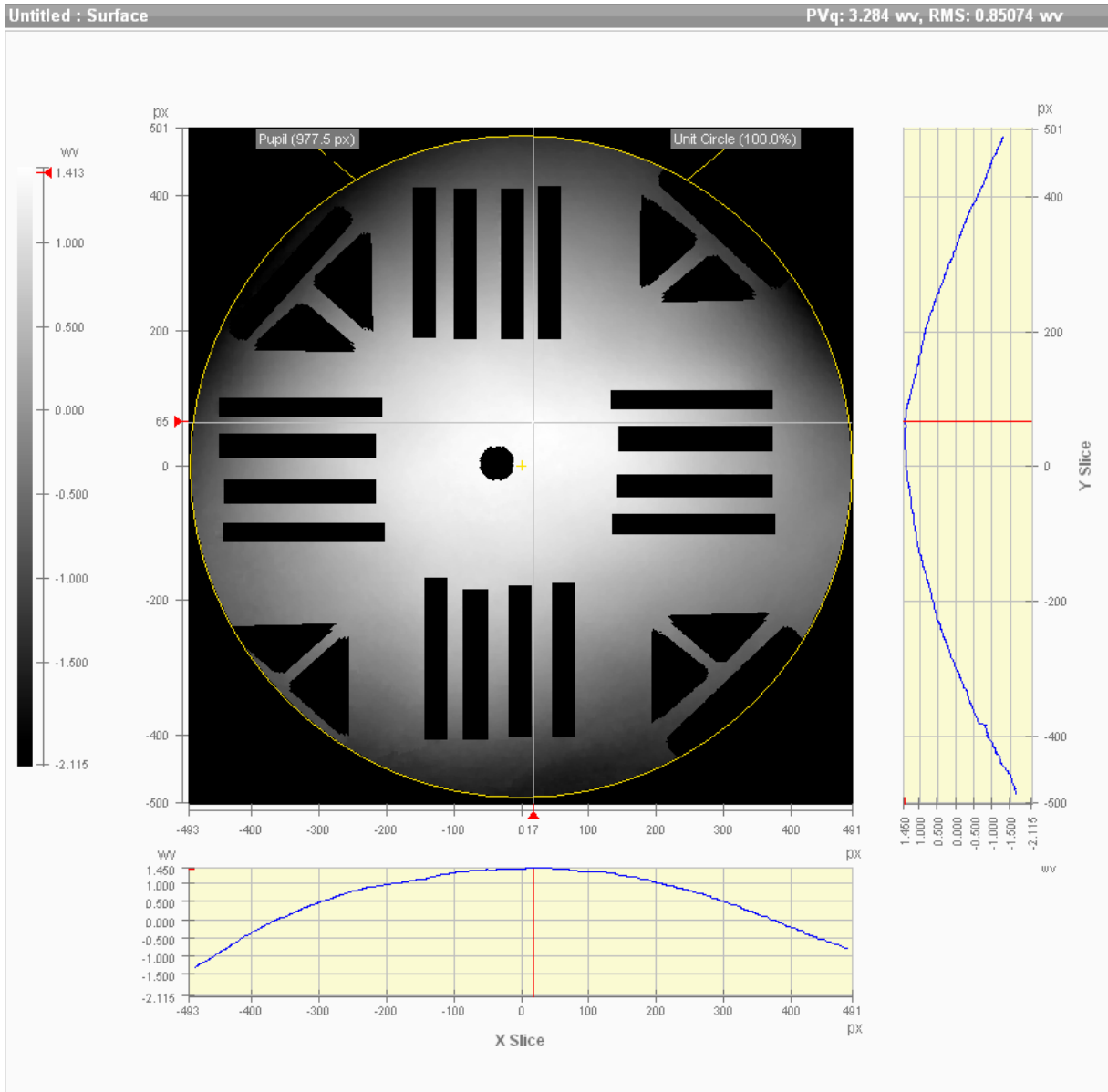


Figure 5: Unwrapped surface obtained from measurement of a 1m carbon fiber target

5. CONCLUSION

We have demonstrated a new dynamic phase-shifting electronic speckle pattern interferometer that uses a single frame spatial phase-shifting technique to significantly reduce sensitivity to vibration and enable the use of a high power pulsed laser. The interferometer designed to measure the stability of the James Webb Space Telescope (JWST) backplane, has a total acquisition time of 9ns and enough energy in the illumination to measure meter-class structures. The ability to measure meter-class structures in the presence of vibration was demonstrated by measuring a 1 meter diameter carbon fiber target at a stand-off of 4 meters with the interferometer and the test article placed on different unisolated tables.

-
- ¹ J.C. Dainty, "Topics in applied physics volume 9", Springer Verlag, Berlin, 1984.
- ² S. Nakadate, T. Yatagai, and H. Saito, "Electronic speckle pattern interferometry using digital image processing techniques," Applied Optics Vol. 19, No. 11, p. 1879-1883, 1980.
- ³ K. Creath, "Phase-shifting speckle interferometry," Applied Optics Vol. 24, No. 18, p. 3053-3058, 1985.
- ⁴ R. Smyth, R. Moore, "Instantaneous phase measuring interferometry," Optical Engr. Vol. 23, No. 4, p. 361, 1984.
- ⁵ C. Koliopoulos, "Simultaneous phase shift interferometer," SPIE vol. 1531, p. 119-127, advanced optical manufacturing and testing II, 1991.
- ⁶ B. Barrientos et, al., "Transient deformation measurement with ESPI using diffractive optical element spatial phase-stepping," Fringe, p317-318, Akademie Verlag (1997).
- ⁷ J.E. Millerd and N.J. Brock, US Patent No. 6,304,330 and 6, 522,808 "Methods and apparatus for splitting imaging and measuring wavefronts in interferometry," Oct 16, 2001.
- ⁸ M. Kuchel, "The new Zeiss interferometer," SPIE Vol. 1332, Optical test and metrology III: recent advances in industrial optical inspection, p. 655-663, 1990.
- ⁹ J. Burke, H. Helmers, "Spatial versus temporal phase shifting in electronic speckle-pattern interferometry: noise comparison in phase maps," Applied Optics, Vol. 39, No. 25, p. 4598-4606, 2000.
- ¹⁰ J. Burke, H. Helmers, "Spatial versus temporal phase shifting in electronic speckle-pattern interferometry: noise comparison in phase maps," Applied Optics, Vol. 39, No. 25, p. 4598-4606, 2000.